Journal of Molecular Graphics and Modelling 39 (2013) 126–132

Contents lists available at SciVerse ScienceDirect

Journal of Molecular Graphics and Modelling

journal homepage: www.elsevier.com/locate/JMGM

Can Si-doped graphene activate or dissociate O_2 molecule?

Ying Chen[a], Xiao-chun Yang[b], Yue-jie Liu[a], Jing-xiang Zhao[a,*], Qing-hai Cai[a], Xuan-zhang Wang[a]

[a] Key Laboratory for Photonic and Electronic Bandgap Materials, Ministry of Education, Harbin Normal University, Harbin 150025, China
[b] Department of Chemistry, Tangshan Teachers College, Tangshan 063000, People's Republic of China

ARTICLE INFO

Article history:
Accepted 12 November 2012
Available online 29 November 2012

Keywords:
Si-doped graphene
Oxygen molecule
Density functional theory

ABSTRACT

Recently, the adsorption and dissociation of oxygen molecule on a metal-free catalyst has attracted considerable attention due to the fundamental and industrial importance. In the present work, we have investigated the adsorption and dissociation of O_2 molecule on pristine and silicon-doped graphene, using density functional theory calculations. We found that O_2 is firstly adsorbed on Si-doped graphene by [2+1] or [2+2] cycloaddition, with adsorption energies of −1.439 and −0.856 eV, respectively. Following this, the molecularly adsorbed O_2 can be dissociated in different pathways. In the most favorable reaction path, the dissociation barrier of adsorbed O_2 is significantly reduced from 3.180 to 0.206 eV due to the doping of silicon into graphene. Our results may be useful to further develop effective metal-free catalysts for the oxygen reduction reactions (ORRs), thus greatly widening the potential applications of graphene.

1. Introduction

Fuel cells can convert chemical energy into electric energy with high efficiency and no pollution. Their performance critically depends on the oxygen reduction reactions (ORRs) at the cathode [1]. The platinum (Pt) and its alloy nanoparticles [2] are traditionally used as active electrocatalysts for ORRs. However, Pt-based electrodes suffer from CO deactivation. In addition, the high cost and the limited reserves of Pt in nature [3] have imposed great limitation for its large-scale commercialization. Therefore, searching for inexpensive and effective metal-free catalysts is highly desirable and has become a hot topic recently.

Graphene [4], a monolayer of two-dimensional structure of sp^2-hybridized carbon, exhibits many intriguing properties, such as superior electrical conductivity [5], a large surface area [6], excellent mechanical flexibility [7], and high thermal/chemical stability [8]. The above unique properties render it to have extensive potential applications in electronics [9–11], (bio)sensors [12–15], batteries [16,17], fuel cells [18–22], catalysts supports [23–35], and so on. Among these applications, our interest is in metal-free catalysts: it has been experimentally demonstrated that nitrogen (N)-doped graphene [23–30] could act as an efficient metal-free electrocatalyst for oxygen reduction in fuel cells. For example, Dai and co-workers for the first time reported that N-doped graphene is a promising candidate as metal-free catalysts for oxygen reduction. More interestingly, the authors suggested that the catalytic activity of this kind of graphene-based catalyst is higher than that of current commercial Pt/C catalysts for ORR [23]. Very recently, the B-, P-, S-, BN-codoped graphenes have been shown to exhibit good catalytic activity toward oxygen reduction [31–35]. Theoretically, several groups have reported that doped graphene-based materials can be used to effectively activate or dissociate oxygen molecule [36–42]. For example, Yang et al. have studied the energy barrier of oxygen molecule dissociation on graphene with different types of nitrogen doping [36]. Bao and Xia have independently studied detailed mechanisms of ORR on N-doped graphene surfaces [37–39]. Obviously, tailoring the electronic arrangement of graphene by doping could be a practical strategy for producing significantly improved materials for ORRs in fuel cells.

On the other hand, our recent studies found that silicon (Si)-doped graphene may be also a metal-free catalyst with high activity. For example, Si-doped graphene can be used to reduce N_2O into N_2 or oxide CO into CO_2 [43,44]. Can Si-doped graphene be used as an alternative metal-free catalyst to dissociate O_2 molecule? Through the detailed density functional theory (DFT) calculations of the interaction of O_2 molecule with Si-doped graphene, we showed that the answer is "yes". To our knowledge, no prior theoretical investigations have been reported on this issue. It should be pointed out that Si-doping into other morphology of graphene, such as fullerenes [45–49] and nanotubes [50] have been reported in experiment. Luckily, very recently, Chisholm et al. for the first time experimentally located and identified the Si impurity atoms in the graphene lattice using annular dark-field imaging in a

* Corresponding author. Tel.: +86 451 88060580.
E-mail address: xjz_hmily@yahoo.com.cn (J.-x. Zhao).

1093-3263/$ – see front matter © 2012 Elsevier Inc. All rights reserved.
http://dx.doi.org/10.1016/j.jmgm.2012.11.009

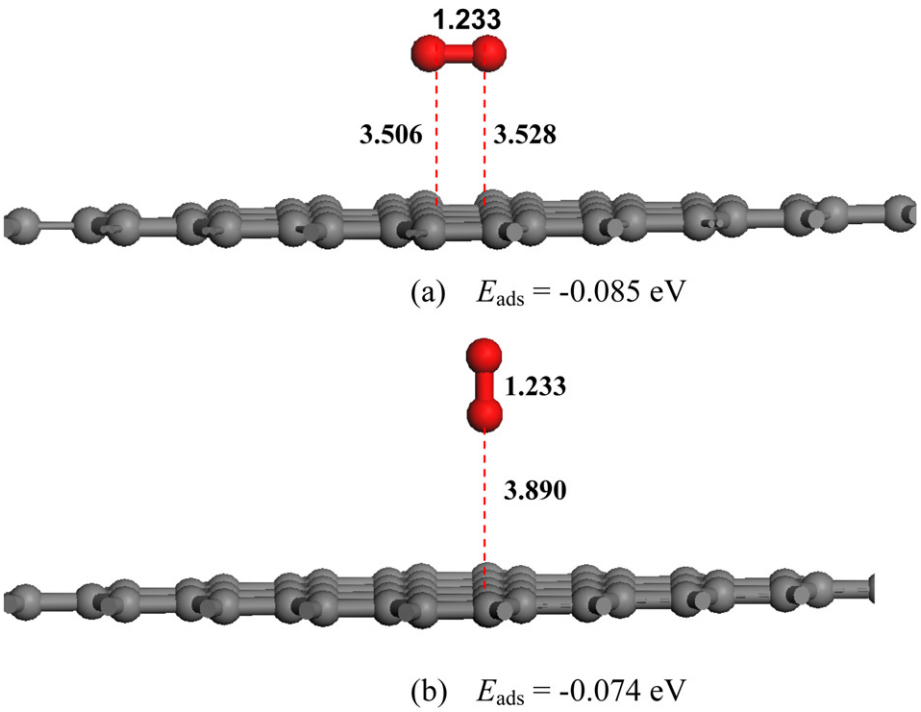

Fig. 1. Optimized configurations for O_2 physisorbed on pristine graphene: (a) parallel site, (b) vertical site. Gray and red balls represent carbon and oxygen atoms, respectively. The bond distances are in angstroms. (For interpretation of the references to color in this figure legend, the reader is referred to the web version of the article.)

scanning transmission electron microscope [51]. This paves the way for the development of Si-doped graphene-based nanodevices.

2. Computational methods and models

We carried out the all-electron ab initio DFT calculations using the spin-polarized generalized-gradient approximation with the Perdew–Burke–Ernzerhof (PBE) [52] functional and the double numerical basis set including polarization function (DNP basis set) implemented in the DMol^3 package [53]. A hexagonal graphene supercell (4×4 graphene unit cells) containing 32 atoms was introduced to model a system with one carbon atom substituted by a silicon atom. The modulus unit cell vector in the z direction was set to 15 Å, which is sufficiently large to avoid the interaction between the graphene and its periodic images. During the geometry optimization without any symmetry constraints, we used $2 \times 2 \times 1$ special k-points to sample the 2D Brillouin zone, while the electronic properties based on the equilibrium structures were computed with $5 \times 5 \times 1$ special k-points. Convergence in energy, force, and displacement was set as 10^{-5} ha, 0.001 ha/Å, and 0.005 Å, respectively. To ensure high-quality results, the real-space global orbital cutoff radius was chosen as high as 4.6 Å in the computations. The smearing of electronic occupations was set as 0.005 ha.

The adsorption energy (E_a) of O_2 molecule on Si-doped graphene was defined as $E_a = E_{total}[Si/graphene + O_2] - E_{total}[Si/graphene] - E_{total}[O_2]$, where E_{total} is the total energy of the calculated systems in the bracket. The charge transfer between Si-doped graphene and the O_2 molecule was analyzed using the Mulliken method. To study the minimum energy pathway (MEP) for O_2 dissociation, linear synchronous transit (LST/QST) and nudged elastic band (NEB) [54] tools in DMol^3 code were used. The vibrational frequencies for each obtained structure along the MEP were calculated at the same level to ensure that every transition state has a single imaginary frequency and the stable local minimum has no imaginary frequency.

3. Results and discussion

3.1. Oxygen adsorption and dissociation on the pristine graphene

First, we have investigated the oxygen adsorption and dissociation on the pristine graphene. Upon adsorption of O_2 molecule on graphene, two adsorption sites are considered as shown in Fig. 1, i.e. O_2 molecule is placed on the graphene with the O—O bond being (i) parallel or (ii) vertical to the graphene surface. The corresponding structural parameters and energetics are shown in Table 1. The results indicate that the interaction of O_2 molecule with the pristine graphene is very weak with adsorption energy of −0.085 eV (labeled as IS, Fig. 1a). Meanwhile, about 0.068 electrons are found to be transferred from graphene to O_2 molecule. Moreover, the distance between pristine graphene and adsorbate is about 3.506 Å. Due to the weak physisorption, it is understandable that the adsorbed O_2 molecule still remains its triplet state.

Moreover, we discuss the dissociation of the adsorbed O_2 molecule on the pristine graphene. The physisorbed oxygen molecule is considered to attack the C—C bond and form a C—O—O—C tetratomic ring. In the transition state (TS, Fig. 2), the

Table 1
Energetic and structural information on the adsorption and dissociation of oxygen on the graphene.

Reaction path		
Physisorption	E_{ads} (eV)	−0.085
	d (Å)	3.506
	d_{O-O} (Å)	1.233
Transition state	E_{ads} (eV)	3.095
	d (Å)	1.407
	d_{O-O} (Å)	2.512
Dissociated	E_{ads} (eV)	2.596
	d (Å)	1.451
	d_{O-O} (Å)	2.856

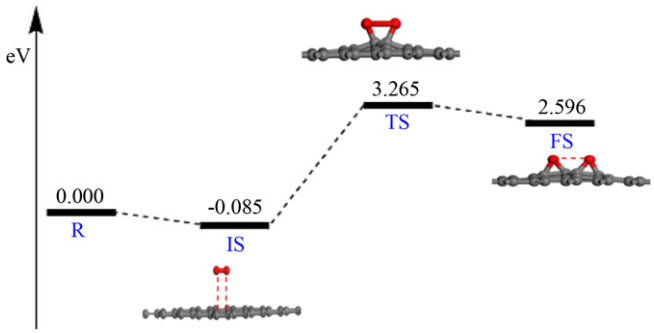

Fig. 2. Minimal energy path of oxygen molecule dissociation on pristine graphene. All energies are given with respect to the reference energy, i.e. the sum of energies of graphene and O_2 molecules, assuming that O_2 and Si-doped graphene are far apart.

C—O bond length is 1.407 Å, indicating that the C—O bond has been achieved. Meanwhile, the distance of O—O increases from 1.233 of IS to 2.512 Å (Table 1). Across this transition state, a product (Fig. 2) is achieved, where the O—O bond has been broken (d_{O-O} = 2.856 Å). Note that an energy barrier of about 3.180 eV has to be overcome and the whole reaction is endothermic by 2.681 eV, which is consistent with previous theoretical calculation [36]. The high barrier and large endothermicity suggest that the dissociation of O_2 molecule on the pristine graphene is unfavorable both dynamically and thermodynamically.

3.2. Oxygen adsorption on Si-doped graphene

When a carbon atom is substituted by a Si atom, the local chemical bonding environment undergoes a substantial change: the bond length between Si-atom and each neighboring C-atom is 1.75 Å, which is much larger than that of the C—C bond of perfect graphene (1.42 Å). The 23% increase in the bond length forces Si-atom to protrude from the graphene plane, also displacing the positions of the neighboring C-atoms out of the plane. The charge analysis using the Mulliken method indicates that about 0.82 e charges are transferred from the silicon atom to the vicinity of the carbon atoms, leading to the partially ionic of the C—Si bonds. For O_2 adsorption on Si-doped graphene, three kinds of initial configurations are considered, including (1) [1 + 1], (2) [2 + 1], and (3) [2 + 2] cycloaddition types. In type (1) the O_2 molecule is vertically attached to the active sites of Si-doped graphene (i.e. Si or its nearest C atoms). In type (2), the O—O bond of O_2 molecule is bound with Si-atom, forming a three-membered ring. In type (3), the O_2 molecule uses its two

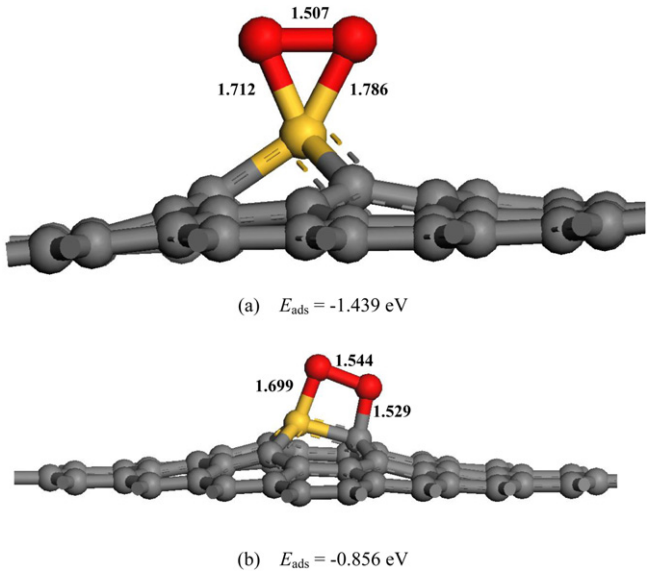

Fig. 3. The calculated stable configurations structures of O_2 on Si-doped graphene: (a) [2 + 1] cycloaddition and (b) [2 + 2] cycloaddition. The yellow ball represents the Si atom. The bond distances are in angstroms. (For interpretation of the references to color in this figure legend, the reader is referred to the web version of the article.)

O-atoms to bond with Si-atom and its neighbor C-atom, leading to the formation of a four-membered ring. Each initial configuration is fully relaxed. Fig. 3 shows the obtained stable configurations of O_2 molecule on Si-doped graphene.

The results suggest that O_2 molecule can chemisorb on the surface of Si-doped graphene. The most energetically favorable configuration is characterized by O_2 parallel to the graphene plane by forming two chemical bonds with Si atom (i.e. type (2)) with the adsorption energy of −1.439 eV (Fig. 3a). The strong chemical interaction renders an increase in O—O length from 1.226 Å to 1.507 Å, while the two Si—O bond lengths are 1.722 and 1.786 Å, respectively, as shown in Fig. 3a. Due to O_2 adsorption, the silicon atom is slightly pulled out of the plane of graphene and the three corresponding C—Si bonds are thus slightly elongated (1.813, 1.813, and 1.837 Å). Moreover, a sizable charge transfer (about 0.736 e) is found from Si-doped graphene to adsorbate. For the most stable configuration, we plot the variation of its total energies with respect to the Si—O_2 distance (Fig. 4a). It is found that the total energies of O_2—Si/graphene increase with the increase of the

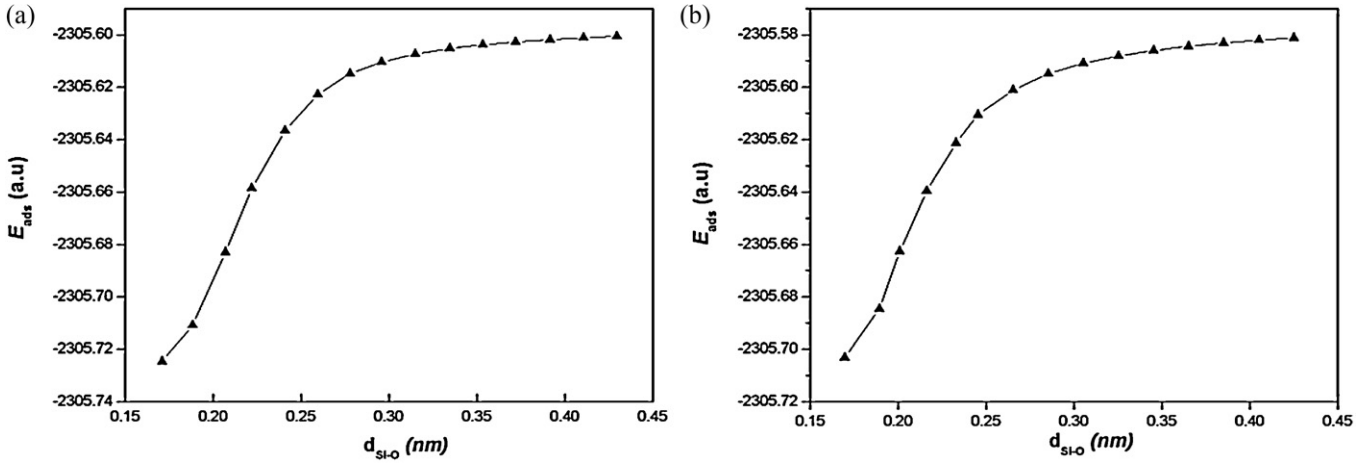

Fig. 4. The variation the total energies of O_2—Si-doped graphene with respect to the average Si—O distance. (a) [2 + 1] cycloaddition and (b) [2 + 2] cycloaddition.

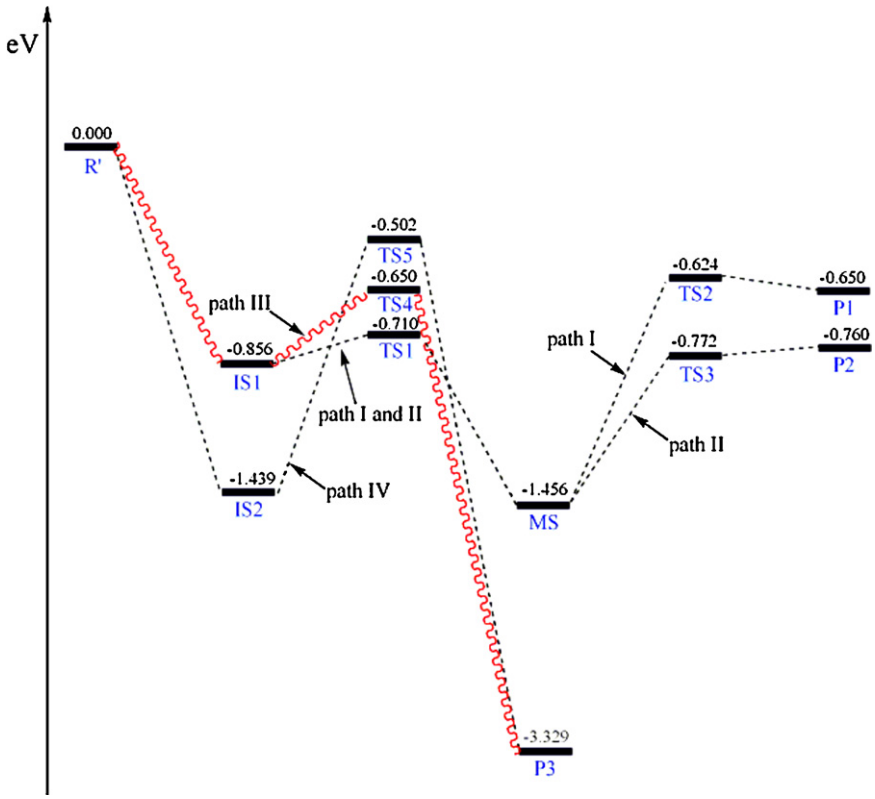

Fig. 5. Schematic energy profile corresponding to local configurations shown in Fig. 6 along the minimum-energy pathway via the $O_2 \rightarrow 2O$ route. All energies are given with respect to the reference energy, i.e. the sum of energies of Si-doped graphene and O_2 molecules.

average Si—O distance. Thus, the O_2 molecule is barrierlessly adsorbed on the Si-doped graphene. In addition, one meta-stable configuration is obtained, in which the O_2 molecule can also be adsorbed on Si-doped graphene by [2+2] cycloaddition with a zero barrier (Fig. 4b). For this configuration (Fig. 3b), the calculated adsorption energy is −0.856 eV and 0.610 electrons are transferred from Si-doped graphene to O_2. The lengths of the new formed Si—O and C—O bonds are 1.699 and 1.529 Å, respectively.

3.3. Reaction mechanisms of O_2 dissociation on Si-doped graphene

The slow ORR kinetics originates from the high strength of the O—O bond and the function of the catalyst is to facilitate the dissociation of that bond. To evaluate the possibility of Si-doped graphene as a candidate for ORR catalyst, we selected the two stable configuration of O_2 molecule on Si-doped graphene as the initial state (IS1 and IS2), where the O_2 molecule is molecularly adsorbed on Si-doped graphene via [2+2] or [2+1] cycloaddition (Fig. 3a and b). The calculated minimum-energy pathway (MEP) profiles along the reaction coordinate are summarized in Fig. 5, where the sum of the energies of the isolated O_2 molecule and clean Si-doped graphene is taken as zero energy. The involved transition states, intermediates, and dissociation products along the reaction path are displayed in Fig. 6, and the corresponding structural parameters are listed in Table 2.

Once O_2 is adsorbed on Si-doped graphene via [2+2] cycloaddition (IS1), two possible paths (labeled as I and II) are proposed for its dissociation, i.e. the two O atoms located at the same or different hexagonal ring. The corresponding products are labeled as P1 and P2, which is characterized as the formation of two three-membered rings. Moreover, to achieve the P3, two other paths (denoted as III and IV) are addressed, which start from IS1 and IS2. In the P3, one O-atom is adsorbed on the Si top site, while the other is attached to the Si—C bond.

In detailed, for paths I and II, an intermediate state (MS) is found before the O_2 is completely dissociated into P1 or P2. For this MS, the distance between the O1-atom and the Si-atom is about 1.577 Å, while the O2-atom binds with the C—C bond, forming a three-membered ring. The two formed C—O bond lengths are 1.459 and 1.473 Å, respectively. To approach MS, a transition state (TS1) has to be overcome with a small intrinsic barrier of 0.146 eV. Meanwhile, the exothermicity is 0.600 eV in this reaction (IS1 → MS). The reaction can proceed following two paths from MS. In the first path, the O1-atom in MS experiences an endothermic transfer (by 0.806 eV) to form the first product (P1) crossing an energy barrier of 0.832 eV (TS2). Note that the two O-atoms locate at different hexagonal ring in the P1. On the other hand, to achieve P2, a barrier of 0.684 eV has to be overcome and this process is endothermic by 0.696 eV with respect to MS.

The third reaction path involves the process that IS1 transforms into P3 with a small barrier of 0.206 eV (TS4). For P3, the Si—O1, C—O2, and Si—O2 bond lengths are 1.558, 1.329, and 1.694 Å, respectively. In particular, the Si-atom is further pulled away from the graphene surface, where the three C—Si bonds are 1.864, 1.865, and 2.518 Å, respectively. Moreover, it can be obviously seen from Fig. 6 that the O—O bond has dissociated with the bond length of 2.778 Å. In addition, the process of IS1 → P3 is highly exothermic by 2.473 eV, accompanied with transfer of about 1.281 electrons from Si-doped graphene to the two O atoms. On the other hand, starting from IS2, the P3 can also be obtained via a transition state (TS5) with an intrinsic barrier of 0.937 eV. Meanwhile, the exothermicity is about 1.903 eV for this process (IS2 → P3). Overall, among the four reaction paths for $O_2 \rightarrow 2O$, the third path is the most favorable in terms of the low barrier (0.206 eV) and large exothermicity (2.473 eV). Yang et al. [36] have reported that nitrogen doping is an

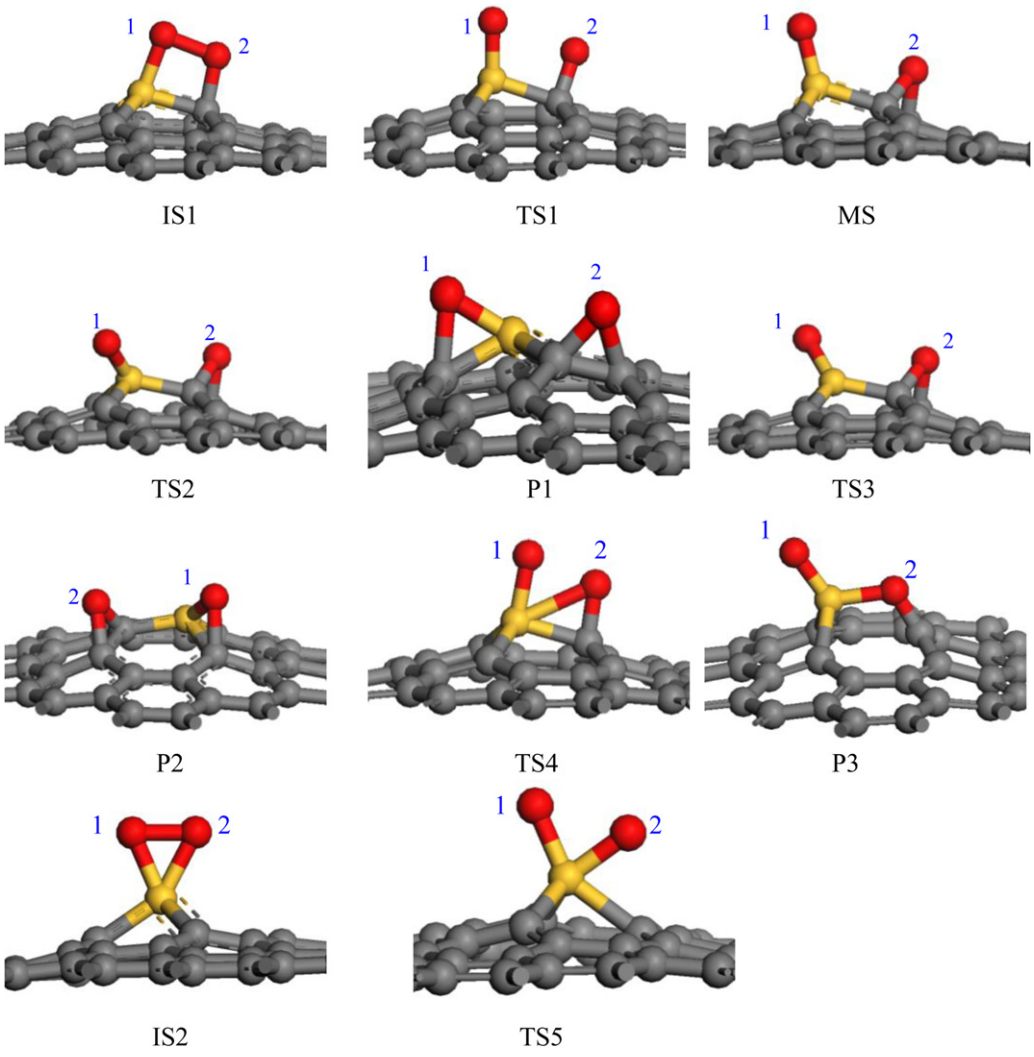

Fig. 6. Local configurations of the adsorbates on the Si-doped graphene at various intermediate states, including the initial state (IS1 and IS2), transition state (TS1, TS2, TS3, TS4, and TS5), metastable state (MS), and final state (P1, P2, and P3) along the minimum-energy pathway via the $O_2 \rightarrow 2O$ route. The yellow and red balls represent the Si and O atom, respectively. The bond distances are in angstroms.

Table 2
Calculated structural parameters of transition states, metastable state, and dissociation products from O_2 adsorbed/dissociated on the Si-doped graphene.

	$d_{(Si–O1)}$ (Å)	$d_{(C–O1)}$ (Å)	$d_{(C–Si)}$ (Å)	$d_{(Si–O2)}$ (Å)	$d_{(C–O2)}$ (Å)		$d_{(O–O)}$ (Å)
TS1	1.587	–	1.847	–	1.410	–	2.382
MS	1.577	–	1.857	–	1.459	1.473	3.260
TS2	1.626	2.065	1.785	–	1.470	1.483	3.699
P1	1.651	1.635	1.789	–	1.471	1.485	3.787
TS3	1.622	1.847	1.822	–	1.451	1.476	3.304
P2	1.651	1.597	1.795	–	1.451	1.479	3.279
TS4	1.667	–	1.841	2.166	1.428	–	1.827
TS5	1.663	–	1.993	1.628	2.171	–	2.060
P3	1.558	–	2.519	1.694	1.329	–	2.778

effective way to decrease the energy barrier of oxygen molecule on graphene and a dissociation barrier of 0.190 eV can be obtained. As compared to the well-established case, the energy barrier of 0.206 eV is small to allow O_2 dissociation on Si-doped graphene. In this sense, we expect that Si-doped graphene is an excellent candidate for the development of a metal-free ORR catalyst.

4. Conclusion

To evaluate the potential of Si-doped graphene in oxygen reduction reactions, we have explored the adsorption and dissociation of O_2 molecule on Si-doped graphene by performing density functional theory calculations. The results indicate that O_2 molecule can be effectively dissociated on Si-doped graphene via a two-step mechanism: (1) molecular chemisorption of O_2 on Si-doped graphene via [2 + 2] or [2 + 1] cycloaddition, followed by (2) the cleavage of the activated O—O bond of O_2. Since the total barrier is very small (0.206 eV) and the exothermicity is enough large (3.329 eV, with respect to the individual O_2 molecule and Si-doped graphene), it is expected that Si-doped graphene can be used as ORR catalysts, which is not suitable for pristine graphene because of the high barrier (3.180 eV) and large endothermicity (2.681 eV). Our

work may be helpful not only to deeply understand the properties of graphene, but also to further develop graphene-based devices.

Acknowledgments

This work is supported by the National Nature Science Foundation of China (Nos. 11074061, 21203048), the University Key Teacher Foundation of Heilongjiang Provincial Education Department (No. 1252G030), the Scientific Innovation Project for Graduate of Heilongjiang Province (No. YJSCX2012-185HLJ), and the Foundation of State Key Laboratory of Theoretical and Computational Chemistry of Jilin University. The authors would like to show great gratitude to the reviewers for raising invaluable comments and suggestions.

References

[1] B.C.H. Steele, A. Heinzel, Materials for fuel-cell technologies, Nature 414 (2001) 345–350.
[2] C. Wang, H. Daimon, Y. Lee, J. Kim, S. Sun, Synthesis of monodisperse Pt nanocubes and their enhanced catalysis for oxygen reduction, Journal of the American Chemical Society 129 (2007) 6974–6975.
[3] M. Winter, R.J. Brodd, What are batteries fuel cells and supercapacitors? Chemical Reviews 104 (2004) 4245–4269.
[4] A.K. Geim, Graphene: status and prospects, Science 324 (2009) 1530–1534.
[5] S.B. Yang, X.L. Feng, S. Ivanovici, K. Müllen, Fabrication of graphene-encapsulated oxide nanoparticles: towards high-performance anode materials for lithium storage, Angewandte Chemie International Edition 49 (2010) 8408–8411.
[6] M.D. Stoller, S.J. Park, Y.W. Zhu, J.H. An, R.S. Ruoff, Graphene-based ultracapacitors, Nano Letters 8 (2008) 3498–3502.
[7] A. Fasolino, J.H. Los, M.I. Katsnelson, Intrinsic ripples in graphene, Nature Materials 6 (2007) 858–860.
[8] A.A. Balandin, S. Ghosh, W.Z. Bao, I. Calizo, D. Teweldebrhan, F. Miao, C.N. Lau, Superior thermal conductivity of single-layer graphene, Nano Letters 8 (2008) 902–910.
[9] K.S. Novoselov, A.K. Geim, S.V. Morozov, D. Jiang, M.I. Katsnelson, I.V. Grigorieva, S.V. Dubonos, A.A. Firsov, Two-dimensional gas of massless Dirac fermions in graphene, Nature 438 (2005) 197–200.
[10] S. Wang, P.K. Ang, Z.Q. Wang, A.L.L. Tang, J.T.L. Thong, K.P. Loh, High mobility, printable, and solution-processed graphene electronics, Nano Letters 10 (2010) 92–100.
[11] C. Lee, X. Wei, J.W. Kysar, J. Hone, Measurement of the elastic properties and intrinsic strength of monolayer graphene, Science 321 (2008) 385–390.
[12] Schedin, A.K. Geim, S.V. Morozov, E.W. Hill, P. Blake, M.I. Katsnelson, K.S. Novoselov, Detection of individual gas molecules adsorbed on graphene, Nature Materials 6 (2007) 652–660.
[13] J.D. Fowler, M.J. Allen, V.C. Tung, Y. Yang, R.B. Kaner, B.H. Weiller, Practical chemical sensors from chemically derived graphene, ACS Nano 3 (2009) 301–310.
[14] C.H. Lu, H.H. Yang, C.L. Zhu, X. Chen, G.N.A. Chen, A graphene platform for sensing biomolecules, Angewandte Chemie International Edition 48 (2009) 4785–4787.
[15] S. Alwarappan, A. Erdem, C. Liu, C.Z. Li, Probing the electrochemical properties of graphene nanosheets for biosensing applications, Journal of Physical Chemistry C 113 (2009) 8853–8857.
[16] Z.S. Wu, W.C. Ren, L. Xu, F. Li, H.M. Cheng, Doped graphene sheets as anode materials with superhigh rate and large capacity for lithium ion batteries, ACS Nano 5 (2011) 5463–5471.
[17] D.H. Wang, D.W. Choi, J. Li, Z.G. Yang, Z.M. Nie, R. Kou, D.H. Hu, C.M. Wang, L.V. Saraf, J.G. Zhang, I.A. Aksay, J. Liu, Self-assembled TiO_2–graphene hybrid nanostructures for enhanced Li-ion insertion, ACS Nano 3 (2009) 907–910.
[18] B. Seger, P.V. Kamat, Electrocatalytically active graphene–platinum nanocomposites, Journal of Physical Chemistry C 113 (2009) 7990–7995.
[19] R. Kou, Y.Y. Shao, D.H. Wang, M.H. Engelhard, J.H. Kwak, J. Wang, V.V. Viswanathan, C.M. Wang, Y.H. Lin, Y. Wang, I.A. Aksay, J. Liu, Enhanced activity stability of Pt catalysts on functionalized graphene sheets for electrocatalytic oxygen reduction, Electrochemistry Communications 11 (2009) 954–960.
[20] E. Yoo, T. Okata, T. Akita, M. Kohyama, J. Nakamura, I. Honma, Enhanced electrocatalytic activity of Pt subnanoclusters on graphene nanosheet surface, Nano Letters 9 (2009) 2255–2259.
[21] Y.C. Si, E.T. Samulski, Exfoliated graphene separated by platinum nanoparticles, Chemistry of Materials 20 (2008) 6792–6797.
[22] Y.M. Li, L.H. Tang, J.H. Li, Preparation and electrochemical performance for methanol oxidation of Pt/graphene nanocomposites, Electrochem. Commun. 11 (2009) 846–850, http://dx.doi.org/10.1016/j.elecom.2009.02.009.
[23] L.T. Qu, Y. Liu, J.-B. Baek, L.M. Dai, Nitrogen-doped graphene as efficient metal-free electrocatalyst for oxygen reduction in fuel cells, ACS Nano 4 (2010) 1321–1326.
[24] S.B. Yang, X.L. Feng, X.C. Wang, K. Müllen, Graphene-based carbon nitride nanosheets as efficient metal-free electrocatalysts for oxygen reduction reactions, Angewandte Chemie International Edition 50 (2011) 5339–5343.
[25] Z.Y. Lin, M.-K. Song, Y. Ding, Y. Liu, M.L. Liu, C.-P. Wong, Facile preparation of nitrogen-doped graphene as a metal-free catalyst for oxygen reduction reaction, Physical Chemistry Chemical Physics 14 (2012) 3381–3387.
[26] I.-Y. Jeon, D.S. Yu, S.-Y. Bae, H.-J. Choi, D.W. Chang, L.M. Dai, J.-B. Baek, Formation of large-area nitrogen-doped graphene film prepared from simple solution casting of edge-selectively functionalized graphite and its electrocatalytic activity, Chemistry of Materials 23 (2011) 3987–3992.
[27] R.L. Liu, D.Q. Wu, X.L. Feng, K. Müllen, Nitrogen-doped ordered mesoporous graphitic arrays with high electrocatalytic activity for oxygen reduction, Angewandte Chemie International Edition 49 (2010) 2565–2569.
[28] H.B. Wang, T. Maiyalagan, X. Wang, A review on recent progress in nitrogen-doped graphene: synthesis, characterization and its potential applications, ACS Catalysis 2 (2012) 781–790.
[29] P. Wang, Z.K. Wang, L.X. Jia, Z.L. Xiao, Origin of the catalytic activity of graphite nitride for the electrochemical reduction of oxygen: geometric factors vs. electronic factors, Physical Chemistry Chemical Physics 11 (2009) 2730–2740.
[30] S.-A. Wohlgemuth, R.J. White, M.-G. Willinger, M.M. Titirici, M. Antonietti, A one-pot hydrothermal synthesis of sulfur and nitrogen doped carbon aerogels with enhanced electrocatalytic activity in the oxygen reduction reaction, Green Chemistry 14 (2012) 1515–1523.
[31] Z.-H. Sheng, H.-L. Gao, W.-J. Bao, F.-B. Wang, X.-H. Xia, Synthesis of boron doped graphene for oxygen reduction reaction in fuel cells, Journal of Materials Chemistry 22 (2012) 390–400.
[32] Z.-W. Liu, F. Peng, H.-J. Wang, H. Yu, W.-X. Zheng, J. Yang, Phosphorus-doped graphite layers with high electrocatalytic activity for the O_2 reduction in an alkaline medium, Angewandte Chemie International Edition 50 (2011) 3257–3261.
[33] Z. Yang, Z. Yao, G.F. Li, G.Y. Fang, H.G. Nie, Z. Liu, X.M. Zhou, X.A. Chen, S.M. Huang, Sulfur-doped graphene as an efficient metal-free cathode catalyst for oxygen reduction, ACS Nano 6 (2012) 205–210.
[34] Z. Yao, H.G. Nie, Z. Yang, X.M. Zhou, Z. Liu, S.M. Huang, Catalyst-free synthesis of iodine-doped graphene via a facile thermal annealing process and its use for electrocatalytic oxygen reduction in an alkaline medium, Chemical Communications 48 (2012) 1027–1327.
[35] S.Y. Wang, L.P. Zhang, Z.H. Xia, A. Roy, D.W. Chang, J.-B. Baek, L.M. Dai, BCN graphene as efficient metal-free electrocatalyst for the oxygen reduction reaction, Angewandte Chemie International Edition 51 (2012) 4209–4212.
[36] S. Ni, Z.Y. Li, J.L. Yang, Oxygen molecule dissociation on carbon nanostructures with different types of nitrogen doping, Nanoscale 4 (2012) 1184–1189.
[37] L. Yu, X.L. Pan, X.M. Cao, P. Hu, X.H. Bao, Oxygen reduction reaction mechanism on nitrogen-doped graphene: a density functional theory study, Journal of Catalysis 282 (2011) 183–190.
[38] L.P. Zhang, Z.H. Xia, Mechanisms of oxygen reduction reaction on nitrogen-doped graphene for fuel cells, Journal of Physical Chemistry C 115 (2011) 11170–11176.
[39] L.P. Zhang, J.B. Niu, L.M. Dai, Z.H. Xia, Effect of microstructure of nitrogen-doped graphene on oxygen reduction activity in fuel cells, Langmuir 28 (2012) 7542–7550.
[40] T. Ikeda, M. Boero, S.-F. Huang, K. Terakura, M. Oshima, J.-I. Ozaki, Carbon alloy catalysts: active sites for oxygen reduction reaction, Journal of Physical Chemistry C 112 (2008) 14706–14709.
[41] T. Ikeda, M. Boero, S.-F. Huang, K. Terakura, M. Oshima, J.-I. Ozaki, S. Miyata, Enhanced catalytic activity of carbon alloy catalysts codoped with boron and nitrogen for oxygen reduction reaction, Journal of Physical Chemistry C 114 (2010) 8933–8937.
[42] Y. Okamoto, First-principles molecular dynamics simulation of O_2 reduction on nitrogen-doped carbon, Applied Surface Science 256 (2009) 335–340.
[43] Y. Chen, B. Gao, J.-X. Zhao, Q.-H. Cai, H.-G. Fu, Si-doped graphene: an ideal sensor for NO- or NO_2-detection and metal-free catalyst for N_2O-reduction, Journal of Molecular Modeling 18 (2012) 2043–2054.
[44] J.-X. Zhao, Y. Chen, H.-G. Fu, Si-embedded graphene: an efficient and metal-free catalyst for CO oxidation by N_2O or O_2, Theoretical Chemistry Accounts 131 (2012) 1242.
[45] J.L. Fye, M.F. Jarrold, Structures of silicon-doped carbon clusters, Journal of Physical Chemistry A 101 (1997) 1836–1840.
[46] T. Kimura, T. Sugai, H. Shinohara, Production and characterization of boron- and silicon-doped carbon clusters, Chemical Physics Letters 256 (1996) 269–270.
[47] C. Ray, M. Pellarin, J.L. Lermé, J.L. Vialle, M. Broyer, X. Blase, P. Mélinon, P. Kéghélian, A. Perez, Synthesis and structure of silicon-doped heterofullerenes, Physical Review Letters 80 (1998) 5365.
[48] M. Pellarin, C. Ray, J.L. Lermé, J.L. Vialle, M. Broyer, X. Blase, P. Kéghélian, P. Mélinon, A. Perez, Photolysis experiments on SiC mixed clusters: from silicon carbide clusters to silicon-doped fullerenes, Journal of Chemical Physics 110 (1999) 6927.
[49] N.V. Bulina, V.A. Lopatin, N.G. Vnukova, I.V. Osipova, G.N. Churilov, W. Krätschmer, Arc synthesis of silicon-doped heterofullerenes in plasma at atmospheric pressure, Fullerenes, Nanotubes and Carbon Nanostructures 15 (2007) 395–400.
[50] J. Campos-Delgado, I.O. Maciel, D.A. Cullen, D.J. Smith, A. Jorio, M.A. Pimenta, H. Terrones, M. Terrones, Chemical vapor deposition synthesis of N-, P-, and Si-doped single-walled carbon nanotubes, ACS Nano 4 (2010) 1696–1702.
[51] M.F. Chisholm, G. Duscher, W. Windl, Oxidation resistance of reactivity atoms in grapheme, Nano Letters 12 (2012) 4651–4655.

[52] G. Henkelman, H. Jonsson, Improved tangent estimate in the nudged elastic band method for finding minimum energy paths and saddle points, Journal of Chemical Physics 113 (2000) 9978–9985.
[53] J.P. Perdew, K. Burke, M. Ernzerhof, Generalized gradient approximation made simple, Physical Review Letters 77 (1996) 3865–3868.
[54] B. Delley, An all-electron numerical method for solving the local density functional for polyatomic molecules, Journal of Chemical Physics 92 (1990) 508–510;
B. Delley, From molecules to solids with the DMol^3 approach, Journal of Chemical Physics 113 (2000) 7756–7764.